



# Transposition of a pericardial-derived vascular adipose flap for myocardial salvage after infarct

Carolina Gálvez-Montón<sup>1\*†</sup>, Cristina Prat-Vidal<sup>1†</sup>, Santiago Roura<sup>1</sup>, Jordi Farré<sup>2</sup>, Carolina Soler-Botija<sup>1</sup>, Aida Lluçà-Valldeperas<sup>1</sup>, Idoia Díaz-Güemes<sup>3</sup>, Francisco M. Sánchez-Margallo<sup>3</sup>, Alejandro Arís<sup>4</sup>, and Antoni Bayes-Genis<sup>1,5</sup>

<sup>1</sup>ICREC (Heart Failure and Cardiac Regeneration) Research Program, IGTP, Cardiology Service, Hospital Universitari Germans Trias i Pujol, Ctra. Can Ruti, Camí de les Escoles, s/n, 08916 Badalona, Barcelona, Spain; <sup>2</sup>Networking Biomedical Research Center on Bioengineering, Biomaterials and Nanomedicine (CIBER-BBN), Barcelona, Spain; <sup>3</sup>Jesús Usón Minimally Invasive Surgery Centre, JUMISC, Cáceres, Spain; <sup>4</sup>Cardiac Surgery Service, Hospital de la Santa Creu i Sant Pau, Barcelona, Spain; and <sup>5</sup>Department of Medicine, UAB, Barcelona, Spain

Received 4 January 2011; revised 2 April 2011; accepted 11 May 2011

Time for primary review: 28 days

## Aims

Coronary artery occlusion is associated with the risk of ventricular remodelling, heart failure, and cardiogenic shock. Novel strategies are sought to treat these ominous complications. We examined the effect of a pericardial-derived fat flap secured over an acute infarct caused by coronary occlusion.

## Methods and results

A novel intervention consisting of the pericardial isolation of a vascularized adipose flap and its transposition fully covering acute infarcted myocardium was developed in the swine model of coronary artery ligation ( $n = 52$ ). Left ventricular (LV) ejection fraction and LV end-diastolic and end-systolic volumes were assessed using magnetic resonance imaging (MRI). Infarct size and gene expression analysis were performed on Day 6 and 1 month. Histological changes, collagen volume fraction (CVF), and vascular density were also evaluated on postmortem sections. One month after the intervention, a 18.8% increase in LV ejection fraction ( $P = 0.007$ ), and significant reductions in LV end-systolic ( $P = 0.009$ ) and LV end-diastolic volumes ( $P = 0.03$ ) were found in treated animals compared with the control-MI group. At Day 6, histopathology confirmed a significant infarct size reduction ( $P = 0.018$ ), the presence of vascular connections at the flap-myocardium interface, and less apoptosis in the infarct border zone compared with control animals ( $P < 0.001$ ). Up-regulation of genes involved in cell cycle progression, cellular growth and proliferation, and angiogenesis were identified within the flap.

## Conclusions

Our results indicate that a vascular fat flap exerts beneficial effects on LV function and limits myocardial remodelling. Future studies must confirm whether these findings provide an alternative therapeutic approach for myocardial salvage after infarction.

## Keywords

Infarction • Ventricular function • Cardiovascular surgery • Fibrosis

## 1. Introduction

Rapid and complete reperfusion of the blocked artery following acute myocardial infarction (MI) is critical to minimize myocardial necrosis and optimize cardiac repair.<sup>1</sup> Therapies to lyse the blood clot<sup>2</sup> and revascularize the stenotic arteries<sup>3,4</sup> are effective treatments for acute MI. Nevertheless, frequently before reperfusion can be achieved or even arterial revascularization has been accomplished, cell necrosis initiates a process of adverse ventricular remodelling, leading to chamber dilatation, contractile dysfunction, and eventually cardiogenic shock.<sup>5,6</sup> Cardiogenic shock complicates 7–10% of cases of acute MI

and is associated with a 70–80% mortality rate.<sup>7</sup> Novel therapeutic approaches for this condition are actively sought.

To improve cardiac function recovery after infarction, engineered heart tissue<sup>8–10</sup>, or autologous vascularized tissue flaps may be effective techniques to limit tissue damage. Omentum flaps have been applied to heal anastomoses considered at risk for dehiscence,<sup>11</sup> and the transposition of *latissimus dorsi* covering the left ventricle has been tested in patients with refractory heart failure.<sup>12</sup>

In this study, we transposed a pericardial-derived adipose flap over an infarct-related coronary artery region in pigs. Here, we provide ‘proof of principle’ evidence of histological and functional benefit, as

\* Corresponding author. Tel: +34 93 4978662; fax: +34 93 4978654, Email: cgalvezmonton@gmail.com

† C.G.-M. and C.P.-V. contributed equally to this work.

well as the potential mechanisms of pericardial adipose flap-aided myocardial salvage after acute coronary occlusion.

## 2. Methods

This study was approved by the Animal Experimentation Unit Ethical Committee of the Catalan Institute of Cardiovascular Sciences (ICCC) and complies with all guidelines concerning the use of animals in research and teaching as defined by the *Guide For the Care and Use of Laboratory Animals* (NIH Publication No. 80-23, revised 1996).

### 2.1 Myocardial infarction model

For this study, 52 female crossbreed Landrace X Large White pigs (30–40 kg) were premedicated with azaperone (10 mg/kg, IM; Stresnil<sup>®</sup>, Laboratorios Dr Esteve, Barcelona, Spain) followed by pentobarbital sodium (15 mg/kg, IV; Tiobarbital<sup>®</sup> 1 g, B.Braun, Barcelona, Spain). Animals underwent endotracheal intubation, and anaesthesia was maintained by 2% isoflurane inhalation. Fentanyl (0.75 mg/kg/45 min, IV; Fentanyl<sup>®</sup>, Kern Pharma, Barcelona, Spain) and a 1.5 mg/kg atracurium besylate bolus (Tracrium<sup>®</sup>, GlaxoSmithKline, London, UK) were given during intervention. Acute MI was induced by a double-ligation (Prolene 5/0 W8556 12-S, Ethicon, Inc., Sommerville, NJ, USA) of the first marginal branch of the circumflex artery, 1.5 cm distal from the atrioventricular groove. Transposition of pericardial adipose flap was performed in the treated group within 30 min after MI induction. In control-MI animals, excision and removal of pericardium and fat preceded coronary occlusion. Tulatromicin (2.5 mg/kg, IM; Draxxin<sup>®</sup>, Pfizer Animal Health, Madrid, Spain) was administered at the end of the intervention and a transdermal fentanyl patch was applied to allow analgesic post-operative care (Durogesic<sup>®</sup>, Janssen-Cilag, Madrid, Spain). All surgical procedures were done under monitoring conditions with ECG registration and measures of capnography, pulse oximetry, non-invasive arterial blood pressure and temperature.

Animals were randomly distributed into 6-day ( $n = 6$  control-MI and  $n = 7$  treated) or 1-month ( $n = 17$  control-MI and  $n = 16$  treated) groups after MI. A subgroup of 1-month pigs ( $n = 7$  control-MI and  $n = 6$  treated) underwent magnetic resonance imaging (MRI) at multiple time points (baseline, 2 h and 1 month after MI) to assess functional recovery. Three additional control-sham pigs (no MI induction) were sacrificed at 1 month to account for related fat flap changes.

### 2.2 Pericardial-derived adipose flap intervention

Under sterile conditions, thoracotomy was performed on the fourth left intercostal space to expose the heart, initially covered by the pericardium and pericardial fat (Figure 1A). Using dissection scissors, the pericardial adipose tissue was easily detached, maintaining its vascularization to create the adipose flap (Figure 1B and C). Then, the pericardium was partially excised and the outer surface of the cardiac chambers exposed. After 30 min of MI induction (Figure 1D), myocardium in the affected region became reddish purple and pericardial adipose flap was gently displaced, to fully cover the ischaemic zone (Figure 1E). To secure the flap, edges were sealed to the myocardial healthy zones using 0.1–0.2 mL of cyanoacrylic-based surgical glue (co-monomer of *N*-butyl-2-cyanoacrylate and metacryloxysulpholane; Glubran<sup>®</sup>2, Cardiolink, Barcelona, Spain) (Figure 1F). Figure 1G–K schematically illustrates the sequence of events involved during the pericardial fat flap intervention.

### 2.3 MRI

Cardiac MRI was performed at 1.5 T (Intera, Philips, Best, The Netherlands) using a phased-array cardiac coil by investigators blinded to the treatment arm. All images were acquired in apnoea with ECG gating.

## 2.4 Morphometric, histological, and immunohistochemical analysis

After being premedicated, all animals were sacrificed with an intravenous injection of potassium chloride solution. Left ventricular (LV) infarct size was blindly measured in digitally photographed transverse heart sections from 1 cm distally to coronary ligation. Biopsies from infarct core, infarct border and remote myocardium were taken and fixed in 10% buffered formalin or flash frozen in liquid nitrogen. Masson's Trichrome was performed for the primary histological examination. A polarized light microscope was used to measure collagen types I and III on randomly selected Sirius red-stained sections from both infarct core and remote zones.<sup>13</sup> Vessel area was blindly assessed by measuring Isolectin-B4-stained (Vectors Labs, Peterborough, UK) vessels in infarct core, border, and remote zones from Day 6 and 1-month groups. Moreover, vessel area within the fat flap was analysed: adipose tissue covering the infarct and that in contact with healthy myocardium. Apoptosis was analysed in infarct core and border zones from 6-day group, using an *in situ* cell death detection kit (Roche Diagnostics, Barcelona, Spain). Quantitative morphometric and histological measurements were completed with Image-Pro Plus software (6.2.1 version; Media Cybernetics, Inc., Bethesda, MD, USA).

## 2.5 Microarray gene expression and analysis

To detect changes in gene expression profile due to pericardial adipose flap intervention, 36 paired tissue samples from both groups were analysed: infarct core, remote zone, pericardial flap from treated animals, and pericardial adipose tissue from control-MI. Here, we compared gene expression in control-MI pericardial adipose tissue and transposed flap from treated animals both at 6 days and at 1 month after intervention. Moreover, we analysed gene expression in myocardial infarct tissue from control-MI and treated animals at both indicated time points.

Microarray expression profiles were obtained using the Affymetrix GeneChip<sup>®</sup> Porcine Genome Array (Affymetrix, Santa Clara, CA, USA). Briefly, 200 ng of total RNA from each sample was processed, labelled, and hybridized to GeneChip<sup>®</sup> according to the Affymetrix GeneChip<sup>®</sup> 3' IVT Express Kit User Manual. For functional analysis, lists of differentially regulated probe sets were uploaded into the Ingenuity Pathway Analysis online tool (IPA 8.0, Ingenuity System, Inc., www.ingenuity.com).

## 2.6 Statistical analysis

Data are presented as mean  $\pm$  SEM. All analyses were performed with SPSS (15.0.1 version, SPSS, Inc., Chicago, IL, USA). Differences between groups were compared using Student's *t*-test or one-way ANOVA for multiple comparisons, with Tukey's test for the *post hoc* analysis. MRI data were analysed as repeated measures using ANOVA with the Greenhouse–Geisser correction. Values of  $P < 0.05$  were considered significant. Microarray data analysis was performed using R and Bioconductor, with an RMA-normalization and non-specific filtering, and limma (linear models for microarray data) package with the false discovery rate correction for the detection of differentially expressed genes.

## 3. Results

Six out of 52 infarcted pigs died during MI induction (4 due to ventricular fibrillation and 2 asystole). No atrial or ventricular arrhythmias were detected during intervention in surviving animals. In all treated pigs, cardiac examination upon sacrifice showed the fat flap covering the infarct area. Serial blood samples were obtained for cardiac biomarkers to measure acute myocardial damage. Remarkably, no significant differences in the circulating levels of cardiac troponin I (cTnI) and myoglobin were found between treated and control-MI animals ( $0.9 \pm 0.2$  vs.  $0.7 \pm 0.3$   $\mu\text{g/L}$ ,  $P = 0.56$ ; and  $451.7 \pm 101.2$  vs.  $425.3 \pm 87.7$   $\mu\text{g/L}$ ,  $P = 0.85$ , respectively).

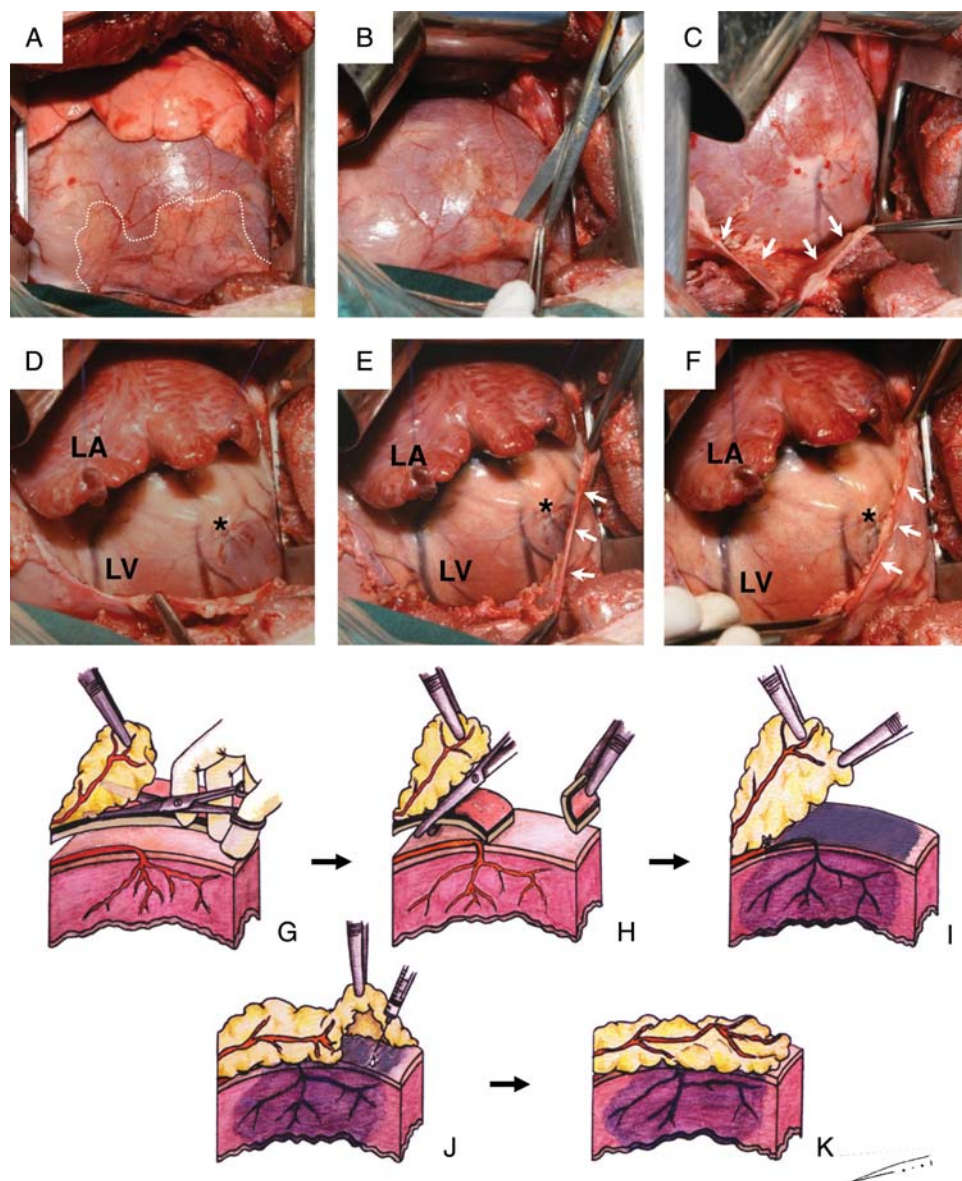


**Figure 1** Pericardial-derived adipose flap intervention. (A) A left thoracotomy exposes the heart and permits fat identification (dotted line). (B and C) Pericardial adipose tissue is dissected to create the flap (arrows). (D) After partial pericardiectomy, MI is performed by a coronary artery ligation (asterisk). (E and F) The pericardial adipose flap is transposed onto the infarct area and the flap glued on healthy edges, covering the ischaemic myocardium. (G–K), Schematic illustrations of the steps involved in pericardial flap intervention are shown. Left atrium (LA); left ventricle (LV).

### 3.1 Ventricular function

Baseline left ventricular ejection fraction (LVEF) was similar between groups ( $P = 0.49$ ). In control-MI, no significant changes were found between 2 h and 1 month ( $P = 0.24$ ) (Supplementary material online, Table S2). In contrast, the LVEF increased from  $38.9 \pm 5.1\%$  post-MI to  $57.7 \pm 3.4\%$  before euthanasia in treated animals ( $P < 0.001$ ). The LVEF improvement was five-fold higher in treated compared with control-MI animals ( $18.8 \pm 6.3$  vs.  $4.1 \pm 6.2\%$ ;  $P = 0.007$ ) (Figure 2A). Delayed enhancement images, acquired before sacrifice, confirmed infarct size was substantially smaller in treated pigs (Figure 2B).

Analysis of ventricular volumes also showed a beneficial remodelling effect in the adipose flap group. In treated animals, end-systolic volume (ESV) significantly decreased between post-MI and 1 month without significant changes over time in end-diastolic volume (EDV) (Supplementary material online, Table S2). In control-MI pigs, ESV showed tendency to increase and EDV significantly increased between 2 h and 1 month due to adverse LV remodelling (see Supplementary material online, Table S2). Comparison between groups showed significant volume differences over time ( $-9.1 \pm 6.6$  vs.  $4.6 \pm 5.6$  mL;  $P = 0.009$  and  $-9.1 \pm 8.5$  vs.  $4.2 \pm 7.4$  mL;  $P = 0.03$ , for ESV and EDV in treated vs. control-MI, respectively) (Figure 2C and D).

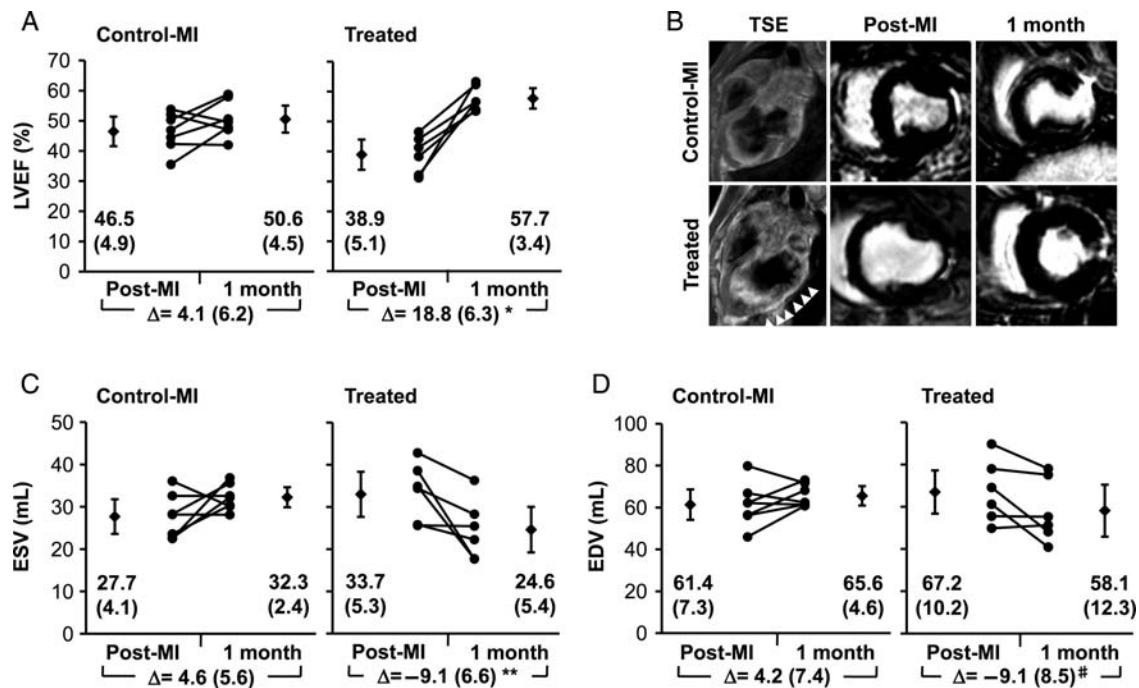


**Figure 2** Cardiac function analysis by MRI. (A) LVEF at 2 h and 1 month after MI in control-MI and treated pigs. Data for individual animals (dots) and mean ( $\pm$  SEM) (diamonds) are shown. (B) Representative turbo-spin-echo (TSE) and T1 short-axis delayed enhancement images for each group. TSE shows, in bright white, the attached adipose flap position in the treated animal (arrowheads). T1 short-axis images reveal healthy (black) and infarcted myocardium (white) at indicated time points. (C and D) End-systolic volume (ESV) and end-diastolic volume (EDV) at 2 h and 1 month post-MI. Data for individual pigs (dots) and mean ( $\pm$  SEM) (diamonds) are represented. (\* $P = 0.007$ , \*\* $P = 0.009$ , and # $P = 0.03$  vs. control-MI group).

### 3.2 Scar maturation and collagen content

A set of experiments was done to analyse gross histopathological changes ( $n = 33$  pigs). Thirteen swine were euthanized 6 days after MI. In control-MI animals, myocardial necrosis involved nearly the full thickness of the ventricular wall in all cases with abundant red blood cell extravasation (Figure 3A). Light microscopy revealed loss of cross striations with appearance of focal hyalinization and interstitial tissue oedema (Figure 3E). In contrast, all treated animals developed non-transmural infarcts (Figure 3B), and only one had scattered zones of macroscopic haemorrhage. Histologically, less oedema and a greater amount of salvaged myocardial tissue was observed in treated animals (Figure 3F). Morphometry revealed that LV infarct area was significantly smaller in treated compared with control-MI pigs ( $5.1 \pm 1.4$  vs.  $12.9 \pm 3.6\%$ ;  $P = 0.018$ ) (Figure 3I).

At 1-month after MI a layer of viable subendocardium (that derives its oxygen directly from the ventricular cavity) was often present in all animals (Figure 3C and D). The necrotic muscle fibres and extravasated red cells were dissolved. At this stage, the infarcted area converted into a firm connective tissue scar in control-MI animals (Figure 3G). Interspersed intact muscle fibres were found more abundantly and LV infarct area was smaller in treated pigs ( $4.4 \pm 2.3$  vs.  $7.7 \pm 3\%$ ;  $P = 0.049$ ) (Figure 3H and J).

Collagen content was measured in infarct core and remote myocardium (Figure 4A–E). On Day 6 after MI, collagen volume fraction (CVF) at the infarct core was  $2.4 \pm 0.4\%$  in treated and  $7.5 \pm 0.5\%$  in control-MI pigs ( $P < 0.001$ ). Collagen type III accounted for only 7% of extracellular matrix in control-MI group while it rose up to 33% of

total collagen in treated animals. At the remote myocardium, CVF was  $0.4 \pm 0.1\%$  in treated and  $1.8 \pm 0.6\%$  in control-MI pigs ( $P = 0.014$ ) (Figure 4E). After 1 month, the mature fibrous scar characteristics were similar among groups (CVF:  $53.7 \pm 14.5$  vs.  $43.8 \pm 13.2\%$ ;  $P = 0.67$ ; collagen type I:  $91.4 \pm 10.8$  vs.  $87.9 \pm 10.8\%$ ;  $P = 0.96$ ; and collagen type III:  $8.6 \pm 10.8$  vs.  $12.1 \pm 10.8\%$ ;  $P = 0.96$ ).

### 3.3 Vascular connections in the flap-myocardium boundary

We studied whether vascularization processes participated in the benefit obtained by the adipose flap. As early as 6 days after treatment, lectin-positive microvessels connecting the vascular flap with the underlying myocardium became apparent (Figure 5A and B). Remarkably, in control-sham pigs (fat flap applied on top on non-infarcted myocardium) these connections were not identified (data not shown). Interestingly, the flap intimately contacting the acutely ischaemic myocardium became intensely vascularized. Vessel area at the flap increased eight-fold compared with unstimulated fat (flap edges covering healthy myocardium) ( $2.4 \pm 0.9$  vs.  $0.3 \pm 0.2\%$ ;  $P < 0.001$ ) (Figure 5C–E). In myocardial tissue samples, comparison of the control-MI and treated group revealed no differences in vessel density in infarct, remote, and border zones at 6 days ( $P = 0.92$ ,  $P = 0.57$ , and  $P = 0.33$ , respectively) and after 1 month ( $P = 0.3$ ,  $P = 0.18$ , and  $P = 0.55$ , respectively).

Increased vascular supply might enhance cell viability. Here, we found at Day 6, a significant reduction in apoptotic cells in the infarct border zone of animals receiving the flap treatment ( $18 \pm$

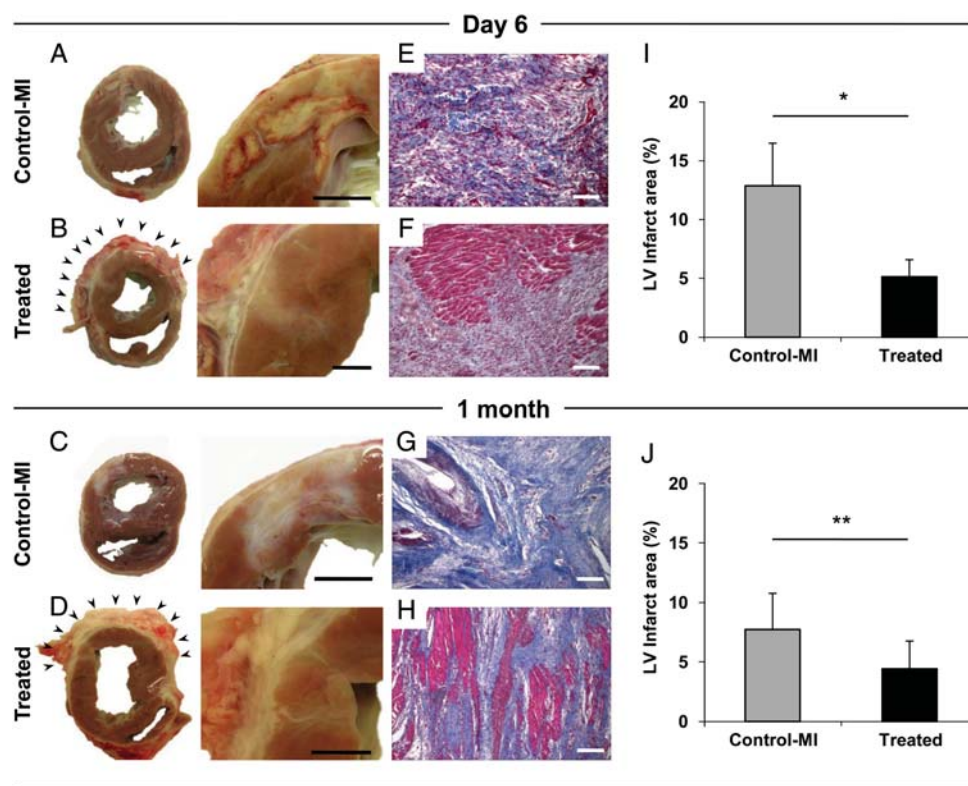


**Figure 3** Morpho-histological analysis. (A–D) Representative photographs of heart sections from control-MI and treated animals of both groups. In treated pigs, the attached pericardial adipose flap is indicated (arrowheads). Enlarged images (scale bar = 1 cm) and Masson's Trichrome staining (E–H) (scale bar = 50  $\mu$ m) of heart slices show the infarct area reduction in treated animals at both time points. (I and J) Percentage of LV infarct area measured in pig hearts both on 6-day and 1-month groups. (\* $P = 0.018$  and \*\* $P = 0.049$ ).

20 vs.  $64 \pm 17\%$ ;  $P < 0.001$ ) (Figure 5F and G). Within the infarct core, a very limited number of cells undergoing apoptosis were identified in both treated (Figure 5I) and control-MI (Figure 5H) animals ( $24 \pm 27$  vs.  $12 \pm 16\%$ ;  $P = 0.4$ ) (Figure 5J).

### 3.4 Gene expression analysis

Finally, we analysed mRNA expression at 6-day and 1-month groups. Of  $\sim 11\,265$  annotated genes interrogated, 81 genes showed differential regulation by the treatment in at least one condition (Figure 6A and B). In the pericardial adipose tissue at Day 6, 13 unique regulated genes were increased and 10 were decreased; at 1 month, 2 unique regulated genes were increased and 13 were decreased; moreover, 10 of the 38 total regulated genes in adipose tissue were altered on both 6-day and 1-month groups (Figure 6A; Supplementary material online, Table S1A–C). Remarkably, all 10 of these common genes, which correspond mostly with transcripts encoding acute phase response proteins, were up-regulated on Day 6 and down-regulated at 1 month (Supplementary material online, Table S1B).

To elucidate which adipokines might participate in the beneficial effect exerted by the flap, we analysed the expression pattern of 56 adipose tissue-related target genes. Comparing stimulated vs. non-stimulated flap, we found 19 related genes interrogated in microarray data, most of them up-regulated (FGF-2, IGF-1, VEGF, TGFB3, TF, IL-18,  $\alpha 2$ -macroglobulin, VCAM-1, ICAM-1, fibronectin, lysyl oxidase, and apelin). Additionally, we only detected VEGF expression by immunohistochemistry in the stimulated-pericardial adipose flap

(see Supplementary material online, Figure S1). In infarct core tissue, 15 unique regulated genes were detected on Day 6; 5 were up-regulated and the remaining down-regulated (Figure 6B; Supplementary material online, Table S1D). At 1 month, 18 unique regulated genes were detected; the majority of them was down-regulated and only 2 were increased (Figure 6B; Supplementary material online, Table S1E). No common genes were found at the two studied time points in infarct core tissue.

Furthermore, IPA identified top genes and functions, and canonical pathways associated with the differentially expressed genes for each comparison analysed. Interestingly, in pericardial adipose tissue, early transcriptional response on Day 6 was dominated by up-regulation of genes involved in cell cycle progression, cellular growth and proliferation, and angiogenesis and blood vessel development (Figure 6C). In addition, those involved in cellular movement and inflammatory response were also up-regulated (Figure 6C).

## 4. Discussion

In this study, we examined the effect of a vascular adipose flap wrapped around oxygen-deprived myocardium in the porcine model. Our data show that a vascularized adipose flap, isolated from the pericardial surface, exerts beneficial effects on LV function. These effects may be partly explained by at least three mechanisms: First, LV volumes were smaller in treated animals, mainly due to reduction in the infarct scar by the flap, and also by direct effects

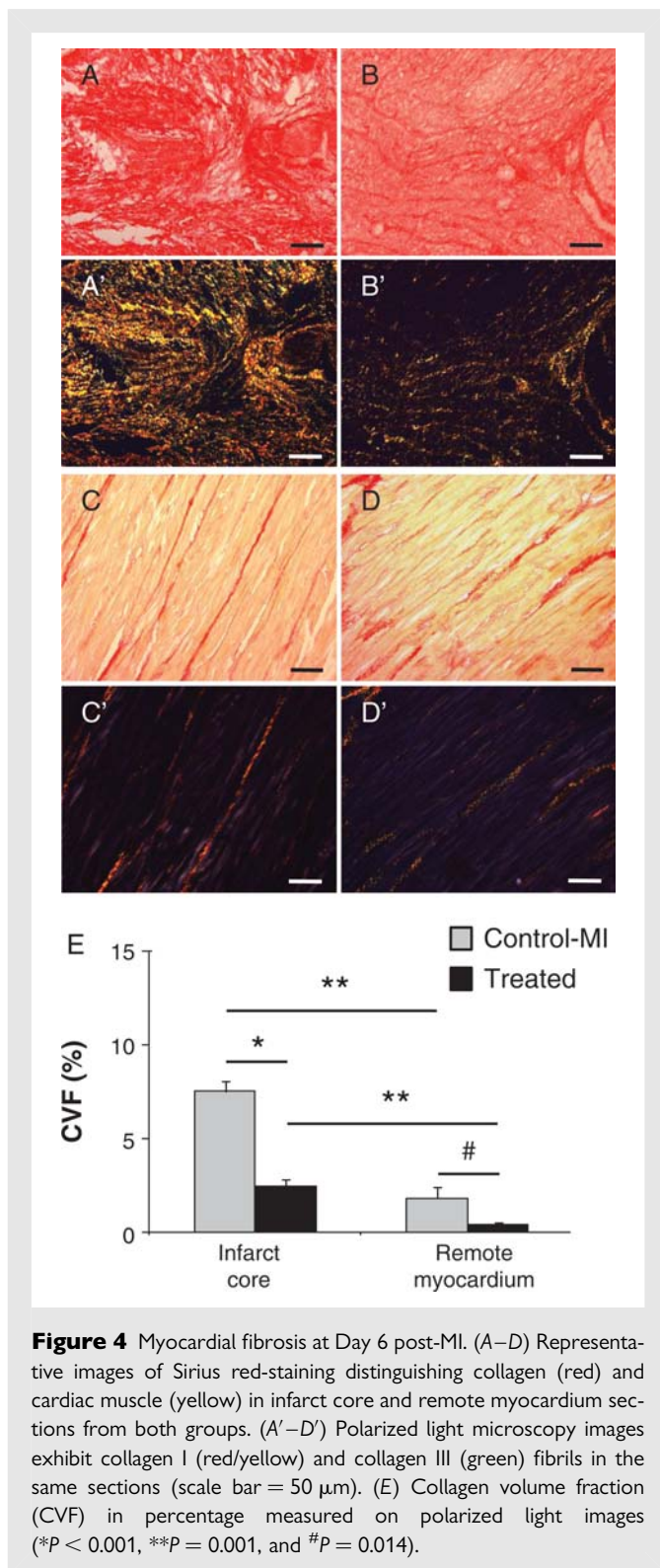


**Figure 4** Myocardial fibrosis at Day 6 post-MI. (A–D) Representative images of Sirius red-staining distinguishing collagen (red) and cardiac muscle (yellow) in infarct core and remote myocardium sections from both groups. (A'–D') Polarized light microscopy images exhibit collagen I (red/yellow) and collagen III (green) fibrils in the same sections (scale bar = 50  $\mu$ m). (E) Collagen volume fraction (CVF) in percentage measured on polarized light images (\* $P$  < 0.001, \*\* $P$  = 0.001, and # $P$  = 0.014).

on the collagen network of the heart. Second, vascular communications developed between the transposed adipose flap and the recipient ischaemic bed. Finally, the former might contribute to cell survival in the infarct border after implantation.

Current techniques used to salvage infarcted myocardium rely on the revascularization of the major epicardial coronary arteries.<sup>3,4</sup> However, the adverse prognosis of cardiogenic shock resulting from acute MI remains a major challenge for cardiologists and

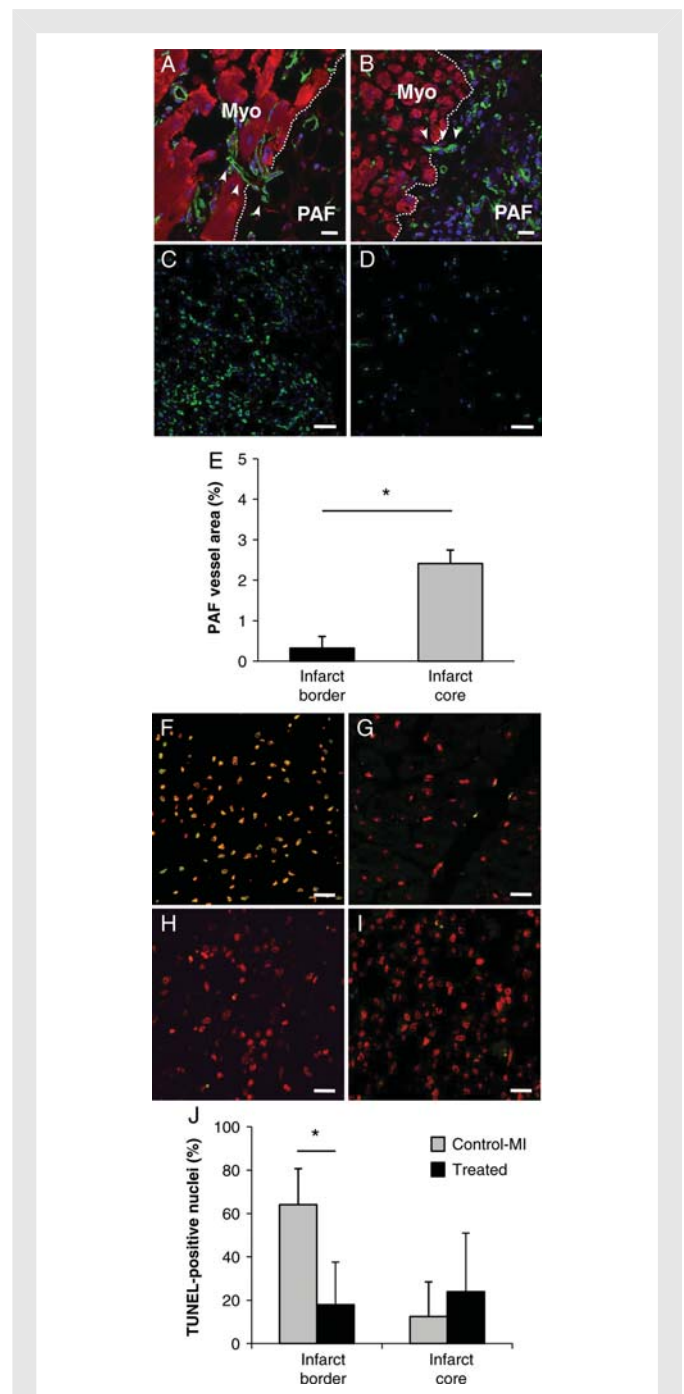


**Figure 5** Microvessels at the fat flap–ischaemic myocardium interface and apoptosis in myocardium 6 days after intervention. (A and B) Immunohistofluorescence against cTnI (red) with Isolectin-B4 (green) and nuclei-Hoechst 33342 (blue) staining shows vascular tubes (arrows) connecting the pericardial adipose flap (PAF) and the myocardium (Myo) boundary (dotted line) (scale bar = 50  $\mu$ m). Representative lectin-stained sections of adipose pedicle stimulated by the ischaemic myocardium (C) and flap edges (D) close to healthy myocardium (scale bar = 20  $\mu$ m). (E) Percentage of vessel area within the flap. Data represent mean ( $\pm$  SEM) of the vessel area occupied per field. (F–I) Representative confocal microscopy images showing TUNEL-positive cells in infarct border (F and G) and infarct core (H and I) from control-MI (F and H) and treated (G and I) animals. The overlaid colour (yellow–orange) corresponds to the sum of TUNEL labelling (green) and the counterstained nuclei (red) (scale bar = 20  $\mu$ m). (J) TUNEL-positive nuclei per field in myocardial zones from both groups. (\* $P$  < 0.001).

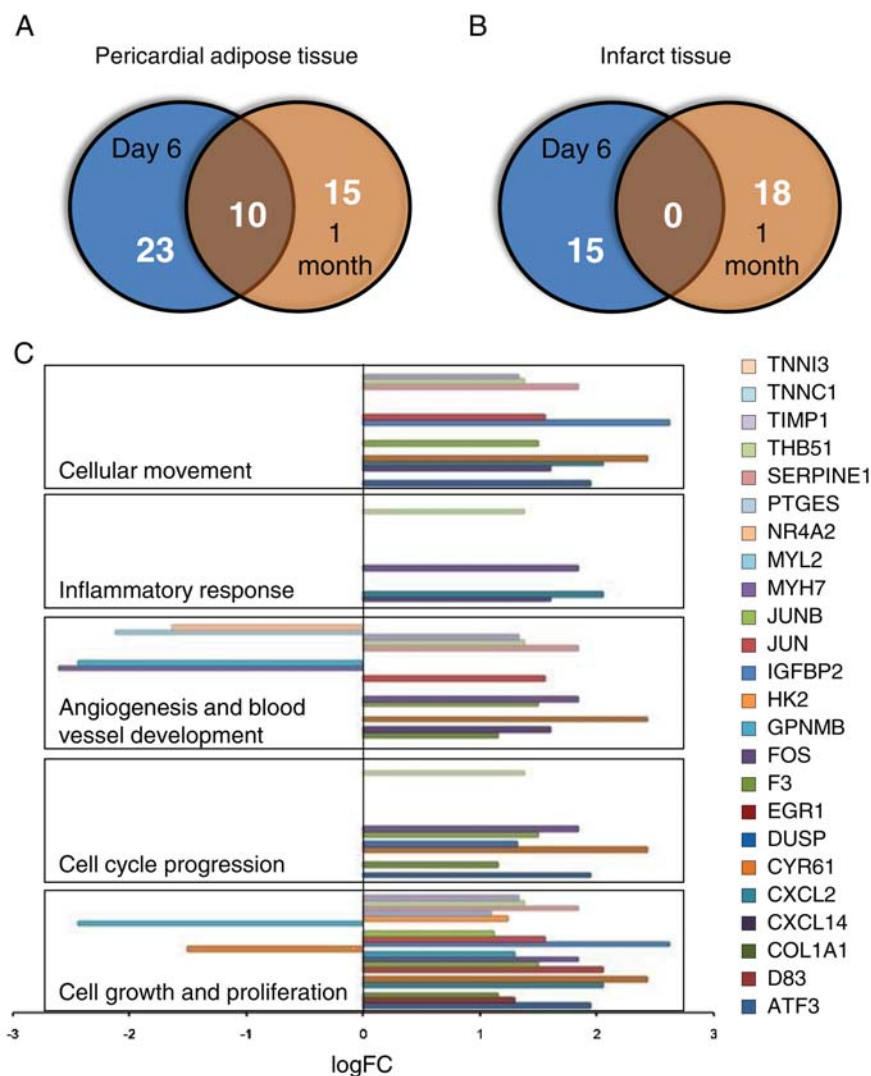


**Figure 6** Pericardial-derived adipose flap intervention alters gene expression. (A and B) Venn diagrams illustrate the number of common and unique regulated genes in pericardial adipose tissue and infarct tissue at Day 6 (blue) and 1 month (orange). Numbers within each circle represent the total number of genes modulated in that experimental condition compared with control-MI group. Only genes differentially expressed ( $P < 0.05$ ) were subjected to Venn analysis. (C) Functions of the top regulated genes in pericardial adipose tissue at Day 6 and the common genes at Day 6 and 1 month. The log FC of the corresponding genes is plotted. Fold change (FC).

cardiovascular surgeons,<sup>6,7</sup> particularly in patients in whom no patent arteries are available for revascularization.<sup>1,14</sup> Over the years, there have been a few efforts to indirectly revascularize the ischaemic heart, including the simple insertion of the internal mammary artery into a hole made in ischaemic myocardium<sup>15</sup> or transmyocardial perforation with lasers to allow perfusion of the ischaemic myocardium, mimicking the sinusoids seen in reptilian hearts.<sup>16</sup> Unfortunately, these methods were either unsuccessful or successful only in selected patients with particular categories of disease.

Dynamic cardiomyoplasty using *latissimus dorsi* muscle was developed to treat congestive heart failure.<sup>17</sup> However, long-term clinical data showed only modest benefit and skeletal muscle fatigue secondary to chronic continuous electrical stimulation. In recent years, there has been a totally innovative approach to surgical treatment of failing myocardium by implanting a mesh wrap around the heart (Acorn

CorCap devices).<sup>18</sup> Despite the promise, the early enthusiasm has been tempered in light of preliminary clinical data.

Indirect revascularization of damaged organs, by means of vascular grafts, has been achieved with more accomplishment.<sup>19,20</sup> Our investigation shows new microvessels develop to bridge the interface between adjacent adipose tissue and ischaemic myocardium. In control-sham animals these vascular connections were not found, thus, demonstrating that tissue injury and hypoxia appear to be strong stimuli for the formation of such collaterals. The temporal stages of blood vessel development have been well described.<sup>21</sup> We already found microvessels on Day 6 after MI at the interface between the pericardial-derived adipose flap and the acutely ischaemic myocardium. Several studies suggest that the invasion of new blood vessels into various tissues occurs within 2–7 days,<sup>22,23</sup> and the time course of angiogenesis in this model is consistent with

those studies. This newly developed collateral circulation may improve local oxygen tension at the flap-myocardium boundary and decrease myocardial tissue hypoxia.

Studies of myocardial samples from patients who died from acute MI show typical apoptotic myocytes, mainly in the border zone of the infarcted myocardium.<sup>24,25</sup> In the present study, we provided further evidence demonstrating that the fat flap intervention improved cardiac function parameters, particularly ejection fraction, and significantly decreased infarct size. These findings in the treated group could be explained by an ischaemic myocardial cell death reduction, as shown in a subgroup of pigs sacrificed early 6 days after coronary artery ligation.

The increment in contractility observed by pericardial adipose flap intervention is far greater than that obtained with other strategies such as stem cell therapy and tissue engineering. A recent meta-analysis of 18 studies and 999 patients concluded that the available evidence suggests bone marrow cell transplantation is associated only with modest improvements in physiological and anatomical parameters (pooled LVEF difference 3.7%).<sup>26</sup> The development of engineered heart tissue for cardiac repair is evolving at a quick pace, yet several important questions remain for its potential clinical application, such as the use of autologous cells with cardiogenic potential and graft immunogenicity.<sup>8,10</sup> Moreover, these engineered approaches have been tested in small rodents with limited benefit in terms of global increase in ejection fraction parameters.<sup>9</sup> Here, we propose an alternative approach using autologous pericardial adipose tissue as a vascularized and biological membrane. In our model, mean global LVEF increased by 19% in the adipose flap group and 4% in the control group. Most importantly, our data were obtained in the swine post-infarction model, the animal model with the highest similarity to the human heart in size and physiology.<sup>27</sup>

Many studies have described the myocardium and perivascular adipose tissue as well-known sources of hormones, which might exert important autocrine, paracrine, and endocrine effects.<sup>28</sup> Such hormones might participate in the early beneficial role of the flap, yet in this study we have not been able to obtain temporal tissue samples in a day to day basis to confirm such effects. However, evidence accumulates that adipose-derived hormones can offer cardioprotective effects against ischaemia, including attenuation of cardiomyocyte apoptosis, reduction in infarct size, and modulation of collagen I/III ratio.<sup>29</sup>

Our results indicate an up-regulation of the potent angiogenic factor VEGF accompanied by hypervascularization only in the infarct-stimulated adipose flap. This is consistent with up-regulation of angiogenic and blood vessel development genes found in the stimulated pericardial adipose flap and with the appearance of vascular communications at the flap-myocardium boundary. We hypothesized that secreted VEGF by adipose tissue has an autocrine effect promoting angiogenesis within the flap. Moreover, a paracrine effect of VEGF in infarcted myocardium might activate the pro-survival Erk 1/2 cascade conferring cardioprotection.<sup>30</sup>

Using polarized light, we were able to detect changes in the structural organization of collagen during scar maturation. The finding of both type I and type III collagen in the scar is consistent with other work on wound healing.<sup>31</sup> The increased amount of type III collagen is typical of the healing process, and the presence of type III fibres is an important feature for subsequent laying down of type I fibres. In animals covered by the adipose flap, we identified more type III fibres at Day 6. The mechanism by which the flap modulates scar

maturation remains elusive; however, modulation of the collagen network may have important implications in the beneficial effect observed by the flap. Myocardial remodelling after infarction is characterized by a change in the proportion of collagens I and III, with an increase in the I/III ratio.<sup>32</sup> Type III collagen provides the framework for the alignment of type I fibres, essential to maintain the shape and contribute to the passive and active stiffness of the myocardium,<sup>33</sup> thus limiting remodelling of the ventricular chambers. Indeed, in our functional experiments, we found less remodelling and less gadolinium retention in treated animals.

Pericardial adipose flap intervention altered gene expression in both myocardial infarct tissue and in the transposed adipose tissue, but only 81 genes appear to be differentially regulated. This may be partially explained by the *P* cut-off criterion which balances sensitivity and specificity in microarray studies.<sup>34</sup> In this study, common altered genes between remote myocardium and infarct core zones were discarded, as well as common genes among healthy adipose tissue and non-treated adipose tissue (control-MI) and/or treated flap. Therefore, our results highlight those genes significantly altered by the treatment irrespective of the infarction itself. Remarkably, in pericardial adipose tissue we found up-regulation of genes involved in angiogenesis and blood vessel development, a finding consistent with the hypervascularization of the stimulated flap and with the appearance of vascular communications at the flap-myocardium boundary.

Coronary artery revascularization is the most effective treatment for acute MI, and all other approaches to salvage myocardium, including the present intervention, may only be considered when revascularization (either by percutaneous or surgical means) is not feasible. One major drawback of this pericardial-derived fat flap intervention, in terms of potential clinical applications, is the need for thoracotomy to gain access to the heart. The use of thoracoscopy for controlled dissection and transposition of the flap would be ideal.

In conclusion, transposition of a pericardial-derived adipose flap exerts beneficial effects on LV function after acute MI in the swine model. The application of a vascularized adipose flap limits LV remodelling, by means of reducing the infarct size and improving cell survival mediated by an enhanced vascular supply. Although we neither observed nor expected complete reversal of myocardial dysfunction after flap engraftment, we believe our study can serve as a proof of principle for a vascular flap approach to salvage cardiac muscle in acute MI.

## Supplementary material

Supplementary material is available at *Cardiovascular Research* online.

## Acknowledgements

We thank T. Bosch and D. Padrol for surgical assistance; C. Díez for support in data analysis; M. Martí and J.R. Lima for their expert technical assistance; J. Maestre, S. Javato, and V. Crisóstomo for helping with MRI execution and analysis; and A. Ferrero for help on statistical analysis.

**Conflict of interest:** none declared.

## Funding

This work was supported by the Instituto de Salud Carlos III, Ministerio de Sanidad y Consumo, [CD07/00163 to C.P.-V.]; Ministerio de Ciencia e

Inovación [SAF2008-05144-C02-01 to A.B.-G.]; La Marató de TV3 [080330 to A.B.-G.]; and from European Comission, 7th Framework Programme [RECATABI, NMP3-SL-2009-229239 to A.B.-G.].

## References

- Antman EM, Anbe DT, Armstrong PW, Bates ER, Green LA, Hand M *et al.* ACC/AHA guidelines for the management of patients with ST-elevation myocardial infarction: a report of the American College of Cardiology/American Heart Association Task Force on Practice Guidelines (Committee to Revise the 1999 Guidelines for the Management of Patients with Acute Myocardial Infarction). *Circulation* 2004;**110**: e82–e292.
- Boersma H, Califf R, Collins R, Deckers JW, Simoons ML. Selection of reperfusion therapy for individual patients with evolving myocardial infarction. *Eur Heart J* 1997; **18**:1371–1381.
- Favaloro RG. Saphenous vein graft in the surgical treatment of coronary artery disease. Operative technique. *J Thorac Cardiovasc Surg* 1969;**58**:178–185.
- Gruntzig A. Transluminal dilatation of coronary-artery stenosis. *Lancet* 1978;**1**:263.
- Cohn JN, Ferrari R, Sharpe N. Behalf of an International Forum on Cardiac Remodeling. Cardiac remodeling—concepts and clinical implications: a consensus paper from an international forum on cardiac remodeling. *J Am Coll Cardiol* 2000;**35**:569–582.
- Hochman JS, Sleeper LA, Webb JG, Sanborn TA, White HD, Talley JD *et al.* Early revascularization in acute myocardial infarction complicated by cardiogenic shock. SHOCK Investigators. Should We Emergently Revascularize Occluded Coronaries for Cardiogenic Shock. *N Engl J Med* 1999;**341**:625–634.
- Goldberg RJ, Gore JM, Alpert JS, Osganian V, de Groot J, Bade J *et al.* Cardiogenic shock after acute myocardial infarction. Incidence and mortality from a community-wide perspective, 1975–1988. *N Engl J Med* 1991;**325**:1117–1122.
- Simpson D, Liu H, Fan TH, Nerem R, Dudley SC Jr. A tissue engineering approach to progenitor cell delivery results in significant cell engraftment and improved myocardial remodeling. *Stem Cells* 2007;**25**:2350–2357.
- Miyahara Y, Nagaya N, Kataoka M, Yanagawa B, Tanaka K, Hao H *et al.* Monolayered mesenchymal stem cells repair scarred myocardium after myocardial infarction. *Nat Med* 2006;**12**:459–465.
- Zimmermann WH, Melnychenko I, Wasmeier G, Didie M, Naito H, Nixdorff U *et al.* Engineered heart tissue grafts improve systolic and diastolic function in infarcted rat hearts. *Nat Med* 2006;**12**:452–458.
- Shrager JB, Wain JC, Wright CD, Donahue DM, Vlahakes GJ, Moncure AC *et al.* Omentum is highly effective in the management of complex cardiothoracic surgical problems. *J Thorac Cardiovasc Surg* 2003;**125**:526–532.
- Magovern JA, Furnary AP, Christlieb IY, Kao RL, Magovern GJ. Right latissimus dorsi cardiomyoplasty for left ventricular failure. *Ann Thorac Surg* 1992;**53**:1120–1122.
- Nicoletti A, Heudes D, Hinglais N, Appay MD, Philippe M, Sassy-Prigent C *et al.* Left ventricular fibrosis in renovascular hypertensive rats. Effect of losartan and spironolactone. *Hypertension* 1995;**26**:101–111.
- Giugliano RP, Braunwald E. Selecting the best reperfusion strategy in ST-elevation myocardial infarction: it's all a matter of time. *Circulation* 2003;**108**:2828–2830.
- Unger EF, Sheffield CD, Epstein SE. Creation of anastomoses between an extracardiac artery and the coronary circulation. Proof that myocardial angiogenesis occurs and can provide nutritional blood flow to the myocardium. *Circulation* 1990;**82**: 1449–1466.
- Stone GW, Teirstein PS, Rubenstein R, Schmidt D, Whitlow PL, Kosinski EJ *et al.* A prospective, multicenter, randomized trial of percutaneous transmyocardial laser revascularization in patients with nonrecanalizable chronic total occlusions. *J Am Coll Cardiol* 2002;**39**:1581–1587.
- Chachques JC, Grandjean P, Schwartz K, Mihaileanu S, Fardeau M, Swynghedauw B *et al.* Effect of latissimus dorsi dynamic cardiomyoplasty on ventricular function. *Circulation* 1988;**78**:III203–III216.
- Jugdutt BI. Current and novel cardiac support therapies. *Curr Heart Fail Rep* 2009;**6**: 19–27.
- Rocha LS, Paiva GR, de Oliveira LC, Filho JV, Santos ID, Andrews JM. Frontal reconstruction with frontal musculocutaneous V-Y island flap. *Plast Reconstr Surg* 2007;**120**: 631–637.
- Motegi S, Tamura A, Abe M, Okada E, Nagai Y, Ishikawa O. Reverse latissimus dorsi musculocutaneous flap for reconstruction of lumbar radiation ulcer. *J Dermatol* 2007;**34**:565–569.
- Folkman J, Klagsbrun M. Angiogenic factors. *Science* 1987;**235**:442–447.
- Morgan E, Lima O, Goldberg M, Ferdman A, Luk SK, Cooper JD. Successful revascularization of totally ischemic bronchial autografts with omental pedicle flaps in dogs. *J Thorac Cardiovasc Surg* 1982;**84**:204–210.
- Pevec WC, Ndoye A, Brinsky JL, Wiltse S, Cheung AT. New blood vessels can be induced to invade ischemic skeletal muscle. *J Vasc Surg* 1996;**24**:534–541; discussion 541–534.
- Saraste A, Pulkki K, Kallajoki M, Henriksen K, Parvinen M, Voipio-Pulkki LM. Apoptosis in human acute myocardial infarction. *Circulation* 1997;**95**:320–323.
- Veinot JP, Gattinger DA, Fliss H. Early apoptosis in human myocardial infarcts. *Hum Pathol* 1997;**28**:485–492.
- Abdel-Latif A, Bolli R, Tleyjeh IM, Montori VM, Perin EC, Hornung CA *et al.* Adult bone marrow-derived cells for cardiac repair: a systematic review and meta-analysis. *Arch Intern Med* 2007;**167**:989–997.
- Weaver ME, Pantely GA, Bristow JD, Ladley HD. A quantitative study of the anatomy and distribution of coronary arteries in swine in comparison with other animals and man. *Cardiovasc Res* 1986;**20**:907–917.
- Ahima RS, Flier JS. Adipose tissue as an endocrine organ. *Trends Endocrinol Metab* 2000;**11**:327–332.
- Sweeney G. Cardiovascular effects of leptin. *Nat Rev Cardiol* 2010;**7**:22–29.
- Hausenloy DJ, Yellon DM. New directions for protecting the heart against ischaemia-reperfusion injury: targeting the Reperfusion Injury Salvage Kinase (RISK)-pathway. *Cardiovasc Res* 2004;**61**:448–460.
- Whittaker P, Boughner DR, Kloner RA. Analysis of healing after myocardial infarction using polarized light microscopy. *Am J Pathol* 1989;**134**:879–893.
- Marijjanowski MM, Teeling P, Mann J, Becker AE. Dilated cardiomyopathy is associated with an increase in the type I/type III collagen ratio: a quantitative assessment. *J Am Coll Cardiol* 1995;**25**:1263–1272.
- Weber KT. Cardiac interstitium in health and disease: the fibrillar collagen network. *J Am Coll Cardiol* 1989;**13**:1637–1652.
- Shi L, Jones WD, Jensen RV, Harris SC, Perkins RG, Goodsaid FM *et al.* The balance of reproducibility, sensitivity, and specificity of lists of differentially expressed genes in microarray studies. *BMC Bioinformatics* 2008;**9**(Suppl. 9):S10.